

## Supplementary Information

### Synthesis of metal-doped nanoplastics and their utility to investigate fate and behavior in complex environmental systems

Denise M. Mitrano\*, Anna Beltzung, Stefan Frehland, Michael Schmiedgruber, Alberto Cingolani, Felix Schmidt

\*Corresponding author information: [denise.mitrano@eawag.ch](mailto:denise.mitrano@eawag.ch)

The supporting information includes the recipe and schematic for PANPd synthesis, digestion protocol, shell feeding mass fraction, conversion of monomer over time, STEM and EDX analysis of all particle variants, table of DLS and zeta potential measurements during leaching experiment, detection limit of nanoplastics in DI water, core stability studies, [Pd] in leaching experiments, evenness of nanoplastic in mixed liquor, photo of settled sludge and proof of concept AF4-MALS-ICP-MS analysis.

Figures: 11

Tables: 2

## ***Polymer synthesis***

The polymerization procedure consisted of a two-step emulsion polymerization, in which first the core particles were synthesized, after which a further shell was grown through feeding a second monomer solution over time (Figure S-1). The use of water-soluble materials was required including surfactants (SDS and KPE), initiator (KPS) and metal precursor ( $\text{K}_2\text{PdCl}_4$ ) which resulted in a chemical entrapment of the metal in the polymer. For all polymerizations, SDS was used for micellar nucleation and the reactor was evacuated and filled with  $\text{N}_2$  (g) three times until it was finally closed to avoid any radical deactivation due to the presence of  $\text{O}_2$  (g). In addition, all synthesis involving AN required the use of an additional surfactant (KPE) to ensure good stability and prevent spontaneous aggregation of the Polyacrylonitrile (abbreviated PAN) nanoparticles inside the reactor.<sup>37</sup> The evolution of the polymer conversion and particle size were followed by thermogravimetric analysis ( $T = 120^\circ\text{C}$ ) using a Mettler Toledo (Switzerland) and by Dynamic Light Scattering (DLS) using a Malvern Zetasizer Nano Z (United Kingdom) with backscatter angle  $173^\circ$  at  $25^\circ\text{C}$ , respectively on an hourly basis (Figure S2 in Supporting Information).

### *Core*

In this first phase the monomer, surfactant and initiator were charged inside the reactor and the dissolved metal precursor was fed into the reaction over the course of two minutes with a simple syringe when the nucleation point was initially achieved. The specified amounts of KPS,  $\text{K}_2\text{PdCl}_4$  and KPE were weighed and added to approximately 8 g of water in separate vials, where they were shaken by hand to ensure complete dissolution of all components (Table S-1). At the outset of the synthesis, the KPE syringe was added at the same pace as the  $\text{K}_2\text{PdCl}_4$ , aiming for a continuous stabilization of the polymer colloids with the addition of the surfactant while at the same time the reaction was being destabilized with the addition of the metal salt, i.e. by screening the charges on the surface of the nanoparticles.

### *Shell*

The previously synthesized core particles acted as a seed for the further growth of the shell. Without stopping the core reaction, an additional 0.18 g of KPS, dissolved in 4 g water, were introduced into the system directly by syringe after which a new feed of monomer mixture is connected to the reaction vessel. Depending on the final morphology of the particle desired, different feed strategies were adopted. In the case of the raspberry particles, a feed of water, styrene and DVB (see CFR in Table 1) was directly connected without any further treatment and left dosing for four hours at a flow rate of 0.06 mL/min. After two hours, an additional 20 g of water was added to the latex solution to reduce solid content and avoid aggregation. The reaction was continually monitored in terms of conversion and particle size, where a conversion rate of monomer to polymer of 90 % or over was established before the reaction was stopped. In the case of the smooth particles, a more gradual change of the feed composition was obtained with the usage of two pumps to provide a gradient between the initial core material (i.e. acrylonitrile) and transition to the styrene outer shell (Figure S-1). An initial feed containing only pure acrylonitrile as monomer was connected to the reactor (CFS\_1, Table S-1) and addition started at 0.06 ml/min. Meanwhile, another flask containing a mixture of water, styrene and DVB (CFS\_2) was dripped into the previous feed, in order to change its composition over a period of three and a half

hours. The gradient actually used in the composition of the feed is reported in Figure S-1, where it is notable that the concentration of styrene and DVB increases over time, while the contribution of acrylonitrile is reduced. Regardless, a constant concentration of monomer is added through the reactor feed (roughly 33 %). Finally, for the remaining one and a half hours of the reaction, the mixture of CFS\_2 was directly used as feed to ensure only styrene was on the outermost shell of the particles. As was the case of the raspberry shell synthesis, after two hours of shell synthesis 20 g water was added to the reaction vessel and constant monitoring of the reaction was performed in terms of particle size (growth) and conversion of monomers.

After the synthesis was complete, the reaction vessel was removed from the oil bath and the latexes were directly filtered with a filter paper (MN 615, 22 s filtration speed) to remove all possible aggregates after the reaction was complete. Finished nanoplastics were stored in plastic bottles at room temperature.

We were successful in upscaling the synthesis to 1 L, with keeping the recipe similar. The only change upon upscaling was to add additional KPS, e.g. 0.5 g in 5 g degassed water, after two hours (half time) of shell feeding.

### ***Microwave Digestion Protocol, Results and Discussion***

Solutions were analyzed by ICP-MS (see main text for details) and in all cases, the calibration curve was matrix matched (DI water or dilute acid). 100% recovery is what would be expected from dilution of the stock material, either PANPd nanoplastics or ionic Pd standards. Direct measurement of the PANPd nanoplastics in DI water matched the expected Pd concentration well given the amount of Pd that was used for synthesis. Several digestion procedures were evaluated to ensure that 1) the digestion protocol would break down the plastics, 2) it would keep the Pd stable in suspension and 3) organic matter would be destroyed. Since the digestion of nanoplastics cannot be easily assessed given their small size, visual confirmation of ability of the procedure to digest plastic was assessed by first attempt to digest microplastic particles with each procedure. Microplastic particles were made by cryogenically milling various neat plastic chips (polystyrene, polypropylene, polyester, low density polystyrene) which were produced in house from raw materials and digestions were made to visually ensure that the digestate was clear after plastic digestion. Digestions were performed with a MLC GmbH ultraCLAVE4. Acids were added undiluted: HNO<sub>3</sub> (65%, SupraPur, Merck), H<sub>2</sub>SO<sub>4</sub> (95-98%), H<sub>2</sub>O<sub>2</sub> (30% w/w in water, Sigma) and HCl (65%, Merck)

The general process for all analyses and digestion goes as follows: the concentrated stock solution was first diluted in DI H<sub>2</sub>O in a polypropylene Falcon tube and then further diluted directly into the measurement tube with appropriate matrix (when no digestion is necessary) or into the digestion tube alongside the matrix. After microwave digestion, the digestate was transferred into a falcon tube with the digestion vessel rinsed with water and added to the falcon tube, followed by ICP-MS analysis. Aqua regia microwave digestion (3:1 HNO<sub>3</sub> to HCl) and reverse aqua regia (1:3 HNO<sub>3</sub> to HCl) were both attempted but did not fully digest the plastic in our initial microplastic tests. HNO<sub>3</sub> and H<sub>2</sub>SO<sub>4</sub> in a ratio of 8:1 was successful in digesting the plastic (4 mL HNO<sub>3</sub> and 0.5 mL H<sub>2</sub>SO<sub>4</sub>), but when an attempt at

WWTP effluent digestion was made a white precipitate, likely fatty acids, were left in suspension. To better dissolve organic matter, 300  $\mu\text{L}$  of  $\text{H}_2\text{O}_2$  was added directly to the complex matrix to begin digestion of the organic matter, with subsequent microwave digestion using the  $\text{HNO}_3$  and  $\text{H}_2\text{SO}_4$  digestion protocol. As  $\text{H}_2\text{O}_2$  reacts with  $\text{H}_2\text{SO}_4$  with off-gassing and bubbling (from formation of perania acid),  $\text{H}_2\text{SO}_4$  was added slowly to the digestion vessel (in 250  $\mu\text{L}$  aliquots) in a fume hood. This procedure was performed in both Teflon and glass digestion vessels to assess if Pd and/or partially digested plastic/Pd remnants stuck to one type of digestion vessel or the other, but recovery was the same in both digestion vessel materials. In both cases, all organic matter was destroyed (i.e. digestate was clear) and for nanoplastic samples a full Pd recovery was achieved. Digestion protocol were also tested with the same concentration of dissolved Pd to as a control to ensure digestion protocol was followed well (i.e. physical transfers between vials, etc.) and that no systematic losses were observed, and these tests, with over 95% Pd recovery, assured us that the Pd (and therefore nanoplastic concentration) was being measured correctly in all subsequent analyses.

Table S-1. Recipe for emulsion polymerization of Pd-containing PAN/poly(ST-DVB) core-shell; 120 g mass synthesis at 10 % polymeric solid content

Core				
Ingredient		Weight %		
Initial Charge	Water <sup>a)</sup>	90		
	SDS <sup>b)</sup>	3		
	Acrylonitrile <sup>a)</sup>	10		
Additional compounds dissolved in water	KPS <sup>b)</sup>	3		
	K <sub>2</sub> PdCl <sub>4</sub> <sup>b)</sup>	1.5		
	KPE <sup>b)</sup>	2		
Shell				
Ingredient		Weight %		
Structure		Raspberry	Smooth	
Feed		CFR	CFS 1	CFS 2
	Water <sup>a)</sup>	66	66	66
	Styrene <sup>a)</sup>	32	1.3	1.3
	Acrylonitrile <sup>a)</sup>	0	33.7	0
	SDS <sup>b)</sup>	2	0	3.1
	DVB <sup>a)</sup>	1	0	1.7

<sup>a)</sup>with respect to total mass, <sup>b)</sup>with respect to monomer



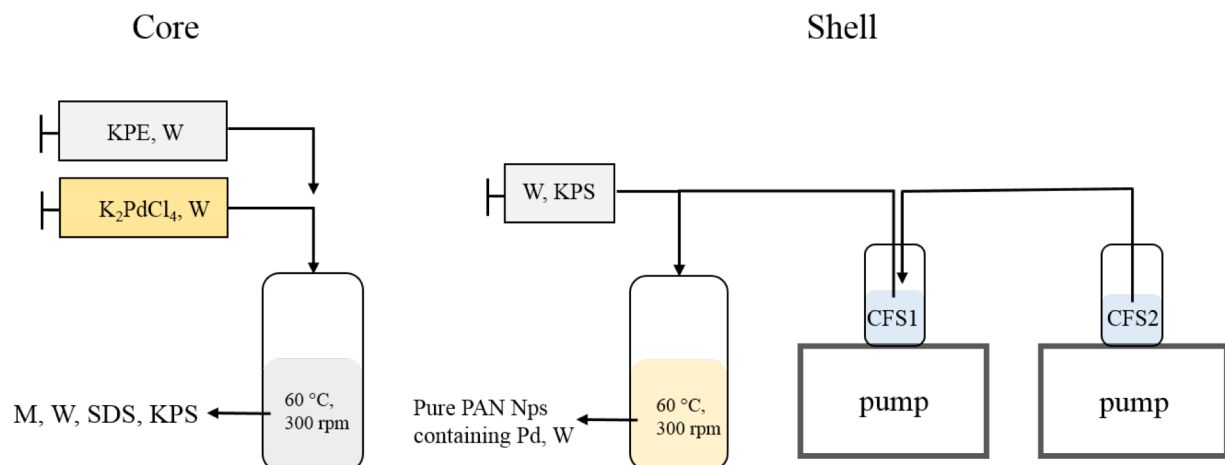


Figure S-1: Schematic representation of the core-shell particle synthesis by conventional batch emulsion for the incorporation of noble metal in polymer nanoparticles (*M* = monomer, *W* = water, *Nps* = nanoparticles). CFS= charge feed shell

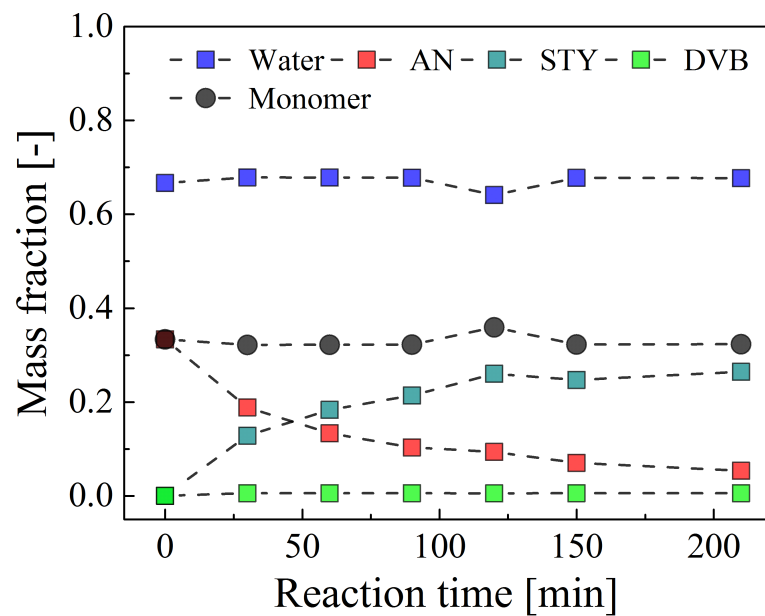


Figure S-2: Gradient in the composition for the feed used for growing the smooth shell.

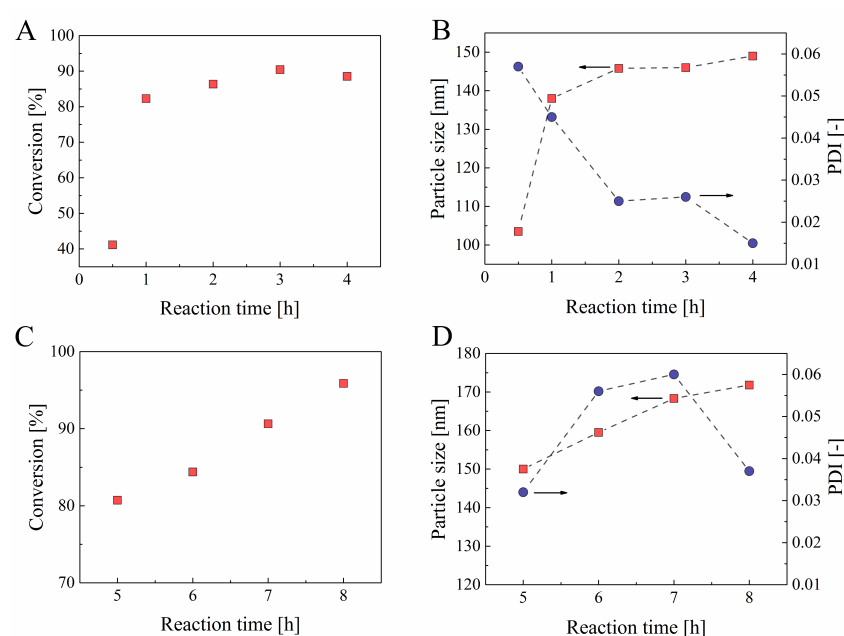


Figure S-3: Conversion of monomer in core (A) and shell (C), as measured by TGA. Particle size evolution of core (B) and shell (D), with corresponding PDI values, as measured by DLS at each hour of synthesis.

The final conversion of monomers to polymer was measured by assessing the amount of residual polymer in the solution and was determined by measuring the solid content of the solution via TGA analysis and comparing this to the theoretical monomer conversion. Typically, the final solid content was approximately 10 wt/wt%. Given the nanoplastic size and the weight percent of polymer in solution, the approximate particle concentration ranged from  $6.22 \times 10^{16}$  to  $8.88 \times 10^{16}$  particles/L. The final weight percent of the Pd in the nanoplastic was calculated to be 0.49%, and so the effective change to the density of the particle given this addition of Pd was minimal. This change in density is not expected to significantly change any intrinsic properties of a latex particle of this size, especially given that the movement of particles under 300 nm are generally expected to be dominated by Brownian motion. Final Pd concentration in the stock solution was approximately 330  $\mu\text{g/L}$  (slight differences depending on batch).

Across multiple syntheses, the average core particle diameter was 100-120 nm in diameter at the time of completion, as measured by SEM with a standard deviation of 1%. After shell addition, the diameter averaged 150-170 nm depending on the batch and when the reaction was stopped, with both smooth and raspberry shells having an overall similar size. DLS measurements (Figure S3) showed slightly larger diameters than when imaging the particles, where the size was found to be  $155 \pm 0.6$  nm,  $159 \pm 0.9$  nm, and  $186 \pm 1.1$  nm for the core, smooth shell, and raspberry shell, respectively. With additional time, the diameter could continue to be grown, though the upper end of the size range possible was not explored. The polydispersity index for all samples was always  $< 0.05$  and, therefore, diameters measured by DLS were the same when measured by intensity weighted or number weighted analysis.

Estimated particle concentrations were achieved by assuming complete monomer conversion during the core synthesis as the mass of latex in solution, the polymer density and radius of the final (core) particle. However, this calculation

derives the maximum number of possible particles in solution, and since the conversion is often less than 100 percent, the particle number in the stock solution is slightly less. Consequently, Pd loading per particle, detection limit and other metrics presented hereafter may be slightly skewed. Obtaining a particle number in solution by direct measurement is often difficult, and all methods are associated with their own amount of uncertainty, and thus our relying on calculation was considered sufficient for these purposes.

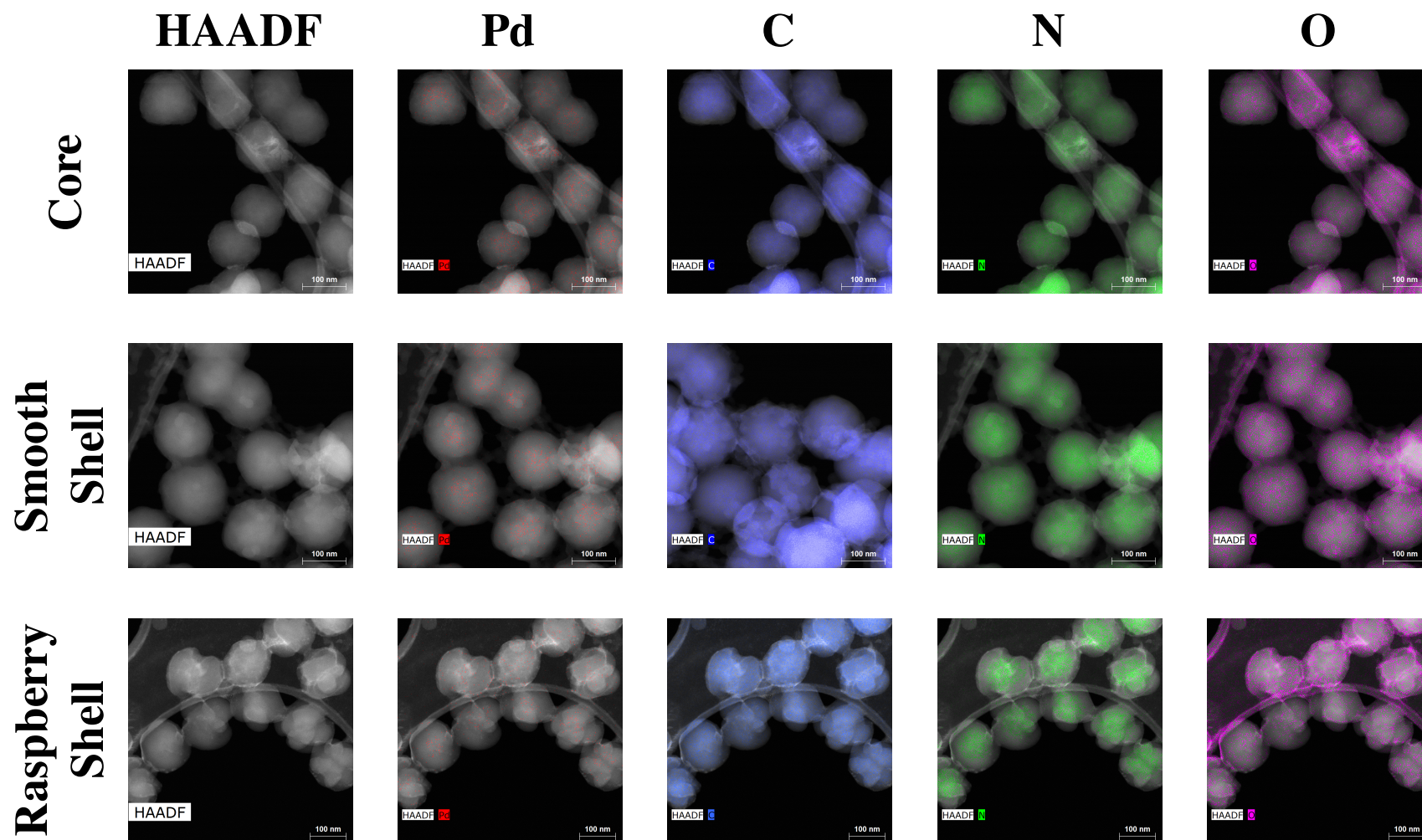


Figure S-4: STEM images of the various synthesis including: PAN core, smooth shell and raspberry shell; all elemental lines enhanced.

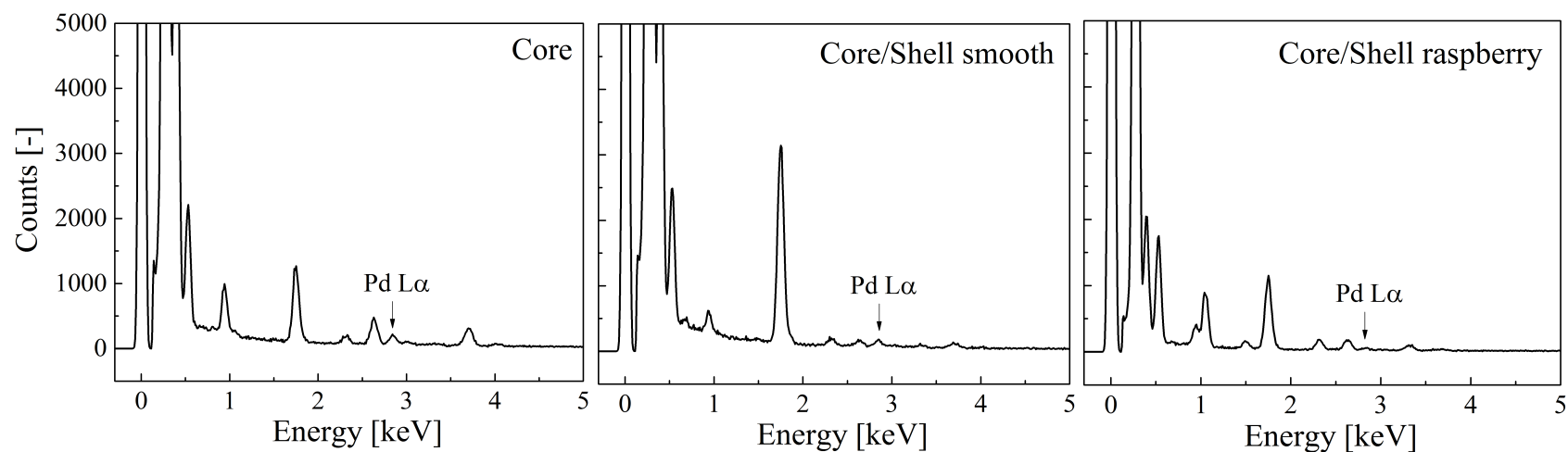


Figure S-5: EDX spectra of STEM images from Figure S3 for PAN core, smooth shell and raspberry shell nanoplastic formulations. The Pd L $\alpha$  is clearly visible in the core particles, with reduced signal in both the particles with an additional shell. The reduced signal is on account that the weight percent of Pd is slightly relatively smaller in the core/shell particles than in the core only particles due to the additional polymer added in the shell building step. However, since both the shell particles used the same core recipe as their base, and corresponding elemental analysis from the ICP-MS shows a similar concentration for all three particle morphologies, the Pd is undoubtedly incorporated into all particles. We can therefore confirm that presence of Pd in the center of the particles as represented in the hypermaps from Figure S3. Other elements of interest, for example N and C, are difficult to distinguish because the bulk of the material is in the lowest energy ranges between 0 and 1 keV; where the K lines for N and C are 0.329 and 0.277 keV, respectively.

Table S-2: DLS (Z-average diameter) and Zeta potential measurements at each weekly time point during leaching experiment. Measurement conducted at approximate particle concentrations of 500  $\mu\text{g/L}$ .

Sample	Time [week]	Size Diameter [nm]	PDI [-]	Surface charge Zeta Potential [mV]
Core	0	$155.5 \pm 0.59$	0.03	$-43.83 \pm 0.45$
	1	$157.4 \pm 2.45$	0.02	$-51.13 \pm 1.16$
	2	$161.2 \pm 0.31$	0.01	$-47.97 \pm 0.12$
	3	$165.8 \pm 0.55$	0.02	$-36.70 \pm 0.35$
	5	$163.0 \pm 1.25$	0.02	$-44.17 \pm 1.24$
	8	$162.4 \pm 0.53$	0.02	$-46.20 \pm 0.50$
Smooth Shell	0	$169.2 \pm 0.50$	0.03	$-56.53 \pm 4.11$
	1	$171.9 \pm 1.45$	0.02	$-52.87 \pm 0.49$
	2	$172.4 \pm 1.35$	0.03	$-50.13 \pm 0.32$
	3	$176.3 \pm 1.32$	0.03	$-50.47 \pm 0.61$
	5	$177.0 \pm 2.15$	0.03	$-43.87 \pm 0.38$
	8	$174.2 \pm 1.30$	0.02	$-45.20 \pm 0.32$
Raspberry Shell	0	$186.6 \pm 1.11$	0.02	$-52.60 \pm 0.50$
	1	$188.1 \pm 1.01$	0.02	$-50.70 \pm 3.48$
	2	$189.3 \pm 1.49$	0.03	$-49.10 \pm 1.35$
	3	$191.9 \pm 0.44$	0.03	$-49.50 \pm 0.26$
	5	$192.3 \pm 1.59$	0.06	$-40.40 \pm 2.29$
	8	$190.3 \pm 1.20$	0.03	$-42.40 \pm 1.02$

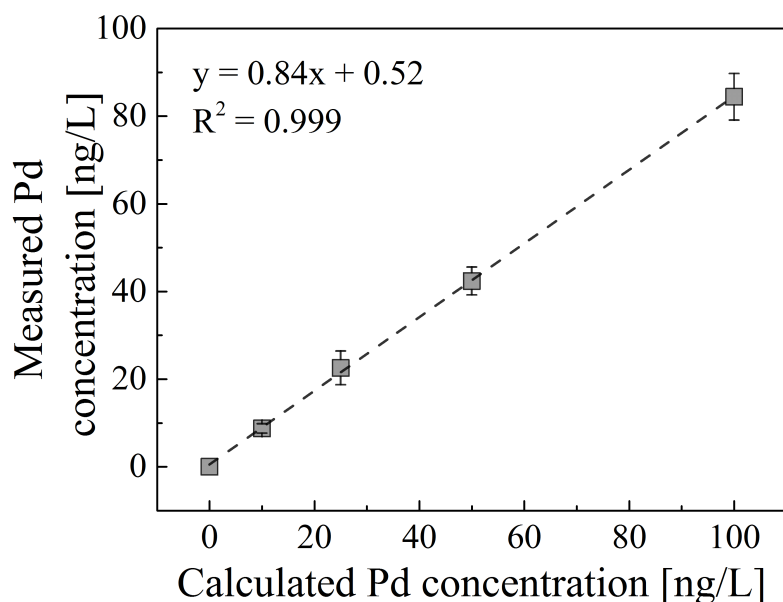


Figure S-6: PANPd particles (smooth shell) measureable at low ng/L Pd concentration. The detection limit measured in DI water was determined to be 5 ng/L Pd, equating to approximately  $9.77 \times 10^8$  particles/L.

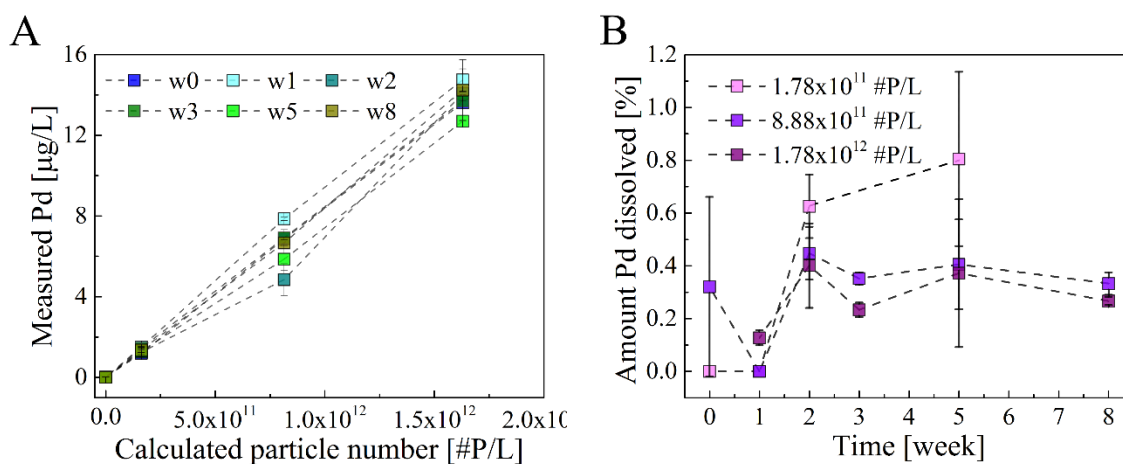


Figure S-7: Nanoplastic particle core only stability (A) and Pd leaching potential (week abbreviated “w”) (B) over time, with particles diluted in DI water and shaking for multiple weeks. See Figure 4 in the main text for final raspberry and smooth shell stability and leaching potential. In the particle core-only solution, there is approximately 0.3% ionic Pd of the total Pd in solution that is not incorporated into the particle at the time of synthesis. While this concentration does rise slightly over the investigated timescale of eight weeks, the leached Pd remains less than 1% and thus the vast majority of Pd that was successfully entrapped in the core at the time of synthesis and remains bound in the nanoplastic particle. However, since the core was not (necessarily) meant to be the final product, the residual Pd in the final core/shell solutions is what is of most interest (see Figure 2 in the main text). This reduction of the free Pd in the syntheses from core synthesis to shell synthesis likely due to the continued incorporation of Pd into the nanoplastics as the shell growth proceeds.

In the core data set, the following outliers were removed: w3 and w8 at  $1.72 \times 10^{11}$  number of particles/L. Moreover, when one out of three measures were below the Pd detection limit of  $0.005 \mu\text{g/L}$ , the average and error of the two remaining valid data were taken.

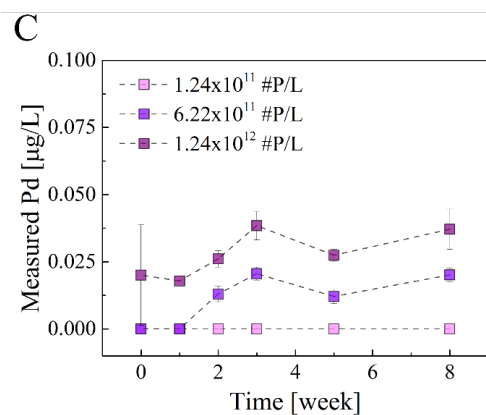
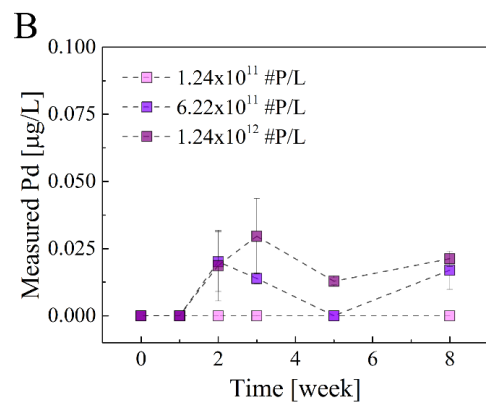
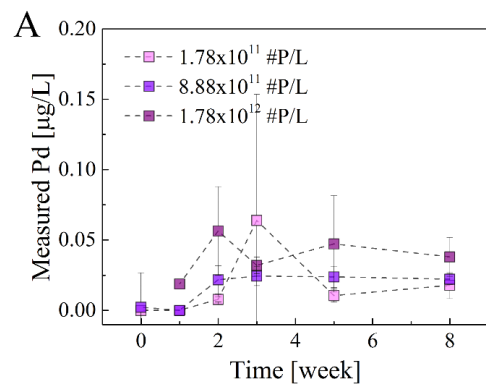


Figure S-8: Measured Pd concentration ( $\mu\text{g/L}$ ) in filtrate from ultracentrifugation (i.e. 10 kDa size cutoff) for PAN core (A), smooth shell (B) and raspberry shell (C).



The experiments involving the detection of Pd in creek water and in WWTP effluent (see Fig. 5 in the main text) were linearly fitted. The corresponding fitting equations and  $R^2$  are listed below:

- For creek water: Fig. 5, panel A) Core:  $y = 0.593x + 0.102$  &  $R^2 = 0.999$ , Smooth:  $y = 0.597x - 0.060$  &  $R^2 = 0.997$ , Raspberry:  $y = 0.602x - 0.056$  &  $R^2 = 0.997$
- For WWTP effluent: Fig. 5, panel (B) Core:  $y = 0.679x - 0.013$  &  $R^2 = 0.999$ , Smooth:  $y = 0.616x - 0.080$  &  $R^2 = 0.994$ , Raspberry:  $y = 0.606x - 0.017$  &  $R^2 = 0.998$

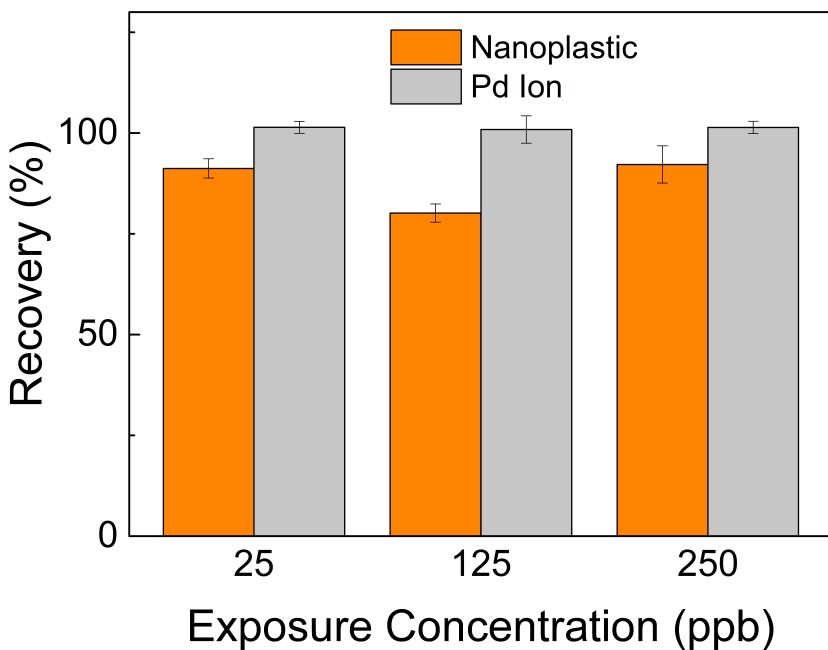


Figure S-9: Recovery of Pd ionic standard (grey) and PANPd particles (orange) spiked into mixed liquor at three exposure concentration, followed by digestion and ICP-MS analysis. A complete recovery of metal and low standard deviation indicates that the material is evenly distributed through the mixed liquor (i.e. no “hotspot” formation) and that sampling protocol gives precise results.



Figure S-10: Experimental set-up for sampling depth profile, mixed liquor settled for 30 min.

### *Adaptability of metal nanometrology techniques for labeled nanoplastics*

#### *Single Particle ICP-MS*

Significant advances have been made in recent years in the field of environmental nanometrology to detect trace concentrations of engineered or natural metal nanoparticles. Some of the most promising techniques, such as single particle inductively coupled plasma mass spectrometry (spICP-MS), can measure metal particles as small as 15 nm in size and at concentrations in the parts per trillion range, even in complex samples. By using the metal fingerprint incorporated into the nanoplastics developed here, the possibility exists to repurpose this nanometrology technique to measure predominantly polymeric materials. For example, a 20 nm pure Au nanoparticle (approximately  $8 \times 10^{-8}$  ng Au/particle) can be readily measured by spICP-MS. While initial attempts were made to measure these nanoplastics via spICP-MS, two factors contributed to not realizing this goal; 1) relatively low Pd incorporation into the nanoplastic and 2) multiple isotopes of Pd which contributed to a decreased detection in spICP-MS mode compared to monoisotopic metals (such as Au). With further refinement, the Pd loading of the current particles (approximately  $5.1 \times 10^{-9}$  ng Pd/particle) could be increased, or if the particle was synthesized with an Au precursor instead, it may be feasible to measure these nanoplastic particles by this ultra-sensitive nanometrology technique. In this case, one would no longer need to measure the aggregate effects or distribution of particulate plastic but could measure individual

nanoplastic particles directly in complex environmental solutions in the same fashion as it has been possible to measure metallic nanoparticles using this method.

*Asymmetrical Flow Field Flow Fractionation(AF4), online size detection (MALS), and elemental analysis (ICP-MS)*

As a proof of concept, Pd-doped nanoplastics in DI water were measured for size and metal content in a hyphenated system. Triplicate samples were run of the smooth shell nanoplastic at a concentration of 500 µg Pd/L. Data presented hereafter are averaged histograms and concentrations. A commercial AF4 (AF2000, Postnova Analytics GmbH, Landsberg, Germany) was connected online to a UV-vis diode array detector (PN3241, Postnova Analytics), a 21-angle MALS detector (PN3621, Postnova Analytics), and a Malvern Zetasizer (Infors, Bottmingen, Switzerland). The AF4 channel was equipped with a 350 µm thick spacer and a 10 kDa PES (polyethersulfone) membrane, which was replaced at the beginning of the experimental set and was sufficient to use for all analysis described herein. Sample injection was performed with an autosampler (PN53000, Postnova Analytics) with a volume of 250 µL (of a 500 µL injection loop). Further fractionation conditions were as follows: 1) 15 min focusing step with an injection flow of 0.2 mL/min, cross flow of 1.5 mL/min and focus flow of 1.8 mL/min, 2) fractionation phase consisting of three steps; a) 0.2 min with cross flow of 1.5 mL/min; constant field, b) 45 min with a cross flow of 1.5 mL/min; power gradient of 0.4, and c) 10 minutes with a cross flow of 0.1 mL/min; constant field, and 3) a 15 min rinse step (i.e. without cross flow but full detector flow) which was applied to minimize the risk of sample carryover. Throughout the entire analysis time, data was collected on-line for UV-vis, DLS and MALS instruments, and fractions were collected automatically using a fraction collector (PN8050, Postnova analytics). The eluent collected represented two min of sample fractionation and thus resulted in a 1 mL sample volume. All individual fractions were diluted for further ICP-MS analysis, in this case 1:10. It should be noted that online coupling of AF4-ICP-MS is also possible. The ICP-MS (Agilent 7500) was tuned daily, calibrated for Pd, and used In as an internal standard during all analysis. For ease of graph reading and because too few particles are being measured during some portions of the run, MALS sizing data is not reported when the particle concentration (as measured by UV) is less than 1% of the highest value recorded.

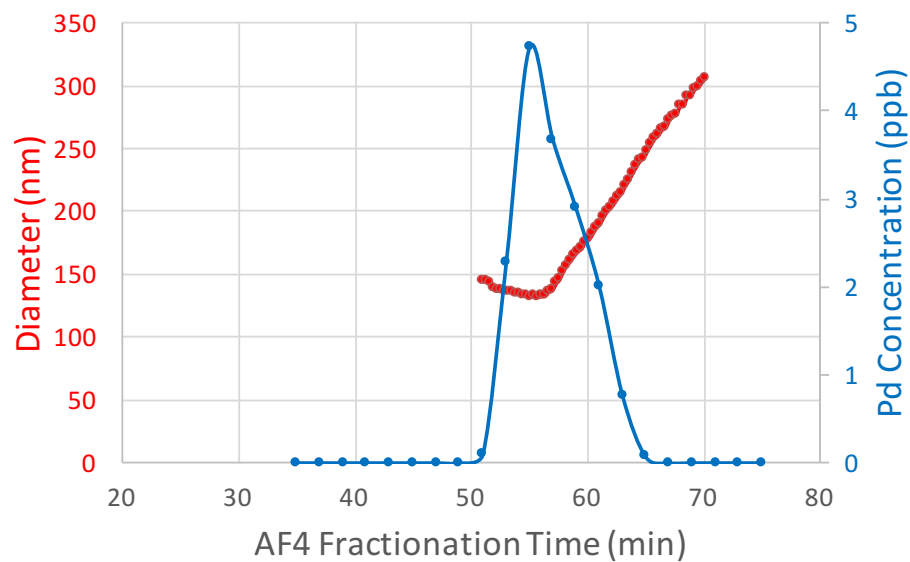


Figure S-11: Smooth shell nanoplastic analysis by AF4-MALS-ICP-MS. On the left (red) y-axis, particle diameter is presented as measured by MALS. On the right (blue) y-axis, this can be compared to Pd concentration, which, as seen in the main body of the manuscript, is directly comparable to particle number.